such terrain corresponds to the low-[H] region around Marcia crater.

The extensive region on Vesta with elevated H content is not plausibly due to a localized enhancement in meteoroid flux or a single isolated impact—for example, fragments of the Veneneia basin impactor. Regolithic howardites such as Kapoeta contain CM, CR, and CI chondrite clasts (*31*) in modest abundance (*12*), which suggests accumulation over time from numerous impactors and asteroidal dust (*36*). Thus, the H-rich region of Vesta probably reflects a zone of more ancient regolith, on which the accumulation of chondritic debris has had a longer history. If Rheasilvia ejecta blanketed this region, it was much thinner than elsewhere on Vesta, so that subsequent gardening has mixed in more of the underlying ancient, carbonaceous chondrite-rich regolith.

The deposition of exogenic material is time-dependent, with H accumulating gradually on exposed surfaces. Accumulation is reset by impact excavation, volatilization, and mantling by ejecta. Thus, the [H] measured with GRaND provides a measure of the relative age of the vestan regolith on a global scale.

References and Notes

1. T. B. McCord, J. B. Adams, T. V. Johnson, *Science* **168**, 1445 (1970).
2. R. P. Binzel, S. Xu, *Science* **260**, 186 (1993).
3. D. W. Mittlefehldt, T. J. McCoy, C. A. Goodrich, A. Kracher, *Rev. Mineral. Geochem.* **36**, 4.1 (1998).
4. M. J. Drake, *Meteorit. Planet. Sci.* **36**, 501 (2001).
5. H. Y. McSween, D. W. Mittlefehldt, A. W. Beck, R. G. Mayne, T. J. McCoy, *Space Sci. Rev.* **163**, 141 (2011).
6. K. Keil, in *Asteroids III*, W. F. Bottke, A. Cellino, P. Paolicchi, R. P. Binzel, Eds. (Univ. Arizona Press in collaboration with the Lunar and Planetary Institute, Tucson, AZ, 2002), pp. 573–584.
7. P. H. Warren, G. W. Kallemeyn, H. Huber, F. Ulff-Møller, W. Choe, *Geochim. Cosmochim. Acta* **73**, 5918 (2009).
8. K. R. Housen, L. L. Wilkening, *Annu. Rev. Earth Planet. Sci.* **10**, 355 (1982).
9. T. H. Prettyman *et al.*, *Space Sci. Rev.* **163**, 371 (2011).
10. T. Usui, H. Y. McSween Jr., D. W. Mittlefehldt, T. H. Prettyman, *Meteorit. Planet. Sci.* **45**, 1170 (2010).
11. C. T. Russell *et al.*, *Science* **336**, 684 (2012).
12. Descriptions of data and methods are available as supplementary materials on *Science* Online.
13. T. H. Burbine, T. J. McCoy, J. L. Hinrichs, P. G. Lucey, *Meteorit. Planet. Sci.* **41**, 1139 (2006).
14. B. E. Clark *et al.*, *J. Geophys. Res.* **109**, (E2), E02001 (2004).
15. E. A. Cloutis *et al.*, *Meteorit. Planet. Sci.* **45**, 1668 (2010).
16. D. W. Mittlefehldt, *Meteorit. Planet. Sci.* **40**, 665 (2005).
17. P. Schenk *et al.*, *Science* **336**, 694 (2012).
18. R. Jaumann *et al.*, *Science* **336**, 687 (2012).
19. E. Asphaug, *Meteorit. Planet. Sci.* **32**, 965 (1997).
20. W. C. Feldman *et al.*, *J. Geophys. Res.* **106**, (E10), 23231 (2001).
21. A. Colaprete *et al.*, *Science* **330**, 463 (2010).
22. M. C. De Sanctis *et al.*, *Science* **336**, 697 (2012).
23. P. C. Thomas *et al.*, *Science* **277**, 1492 (1997).
24. S. Marchi *et al.*, *Science* **336**, 690 (2012).
25. D. W. Mittlefehldt, in *Treatise on Geochemistry*, D. H. Heinrich, K. T. Karl, Eds. (Pergamon, Oxford, 2007), pp. 291–324.
26. R. Bustin, E. K. Gibson Jr., in *The Second Conference on Lunar Bases and Space Activities of the 21st Century*, W. W. Mendell, Ed. (NASA, Washington, DC, 1992), pp. 437–445.
27. L. Schultz, L. Franke, *Meteorit. Planet. Sci.* **39**, 1889 (2004).
28. S. Hasegawa *et al.*, *Geophys. Res. Lett.* **30**, 2123 (2003).
29. A. Rivkin, L. McFadden, R. Binzel, M. Sykes, *Icarus* **180**, 464 (2006).
30. V. Reddy *et al.*, *Science* **336**, 700 (2012).
31. M. E. Zolensky, M. K. Weisberg, P. C. Buchanan, D. W. Mittlefehldt, *Meteorit. Planet. Sci.* **31**, 518 (1996).
32. J. S. Herrin, M. E. Zolensky, J. A. Cartwright, D. W. Mittlefehldt, D. K. Ross, *Proc. Lunar Planet. Sci. Conf.* **42**, 2806 (2011).
33. K. Lodders, B. J. Fegley, *The Planetary Scientist's Companion* (Oxford Univ. Press, New York, 1998).
34. J. F. Kerridge, *Geochim. Cosmochim. Acta* **49**, 1707 (1985).
35. B. Denevi, *Science* (2012).
36. M. Gounelle, M. E. Zolensky, J.-C. Liou, P. A. Bland, O. Alard, *Geochim. Cosmochim. Acta* **67**, 507 (2003).
37. J.-Y. Li *et al.*, *Icarus* **208**, 238 (2010).

Acknowledgments: We thank the Dawn team for spacecraft and instrument operations at Vesta. Portions of this work were performed by the Planetary Science Institute under contract with the Jet Propulsion Laboratory (JPL), California Institute of Technology; by JPL under contract with NASA; and by the NASA Dawn Participating Scientist Program. D. Bazell and P. Peplowski of Johns Hopkins University Applied Physics Laboratory assisted in fast-neutron data analysis. The Dawn mission is led by the University of California, Los Angeles, and managed by JPL under the auspices of the NASA Discovery Program Office. The Dawn data are archived with the NASA Planetary Data System.

Supplementary Materials

www.sciencemag.org/cgi/content/full/science.1225354/DC1
Supplementary Text
Figs. S1 to S27
Tables S1 to S4
References (*38–442*)

29 May 2012; accepted 13 August 2012
Published online 20 September 2012;
10.1126/science.1225354

Pitted Terrain on Vesta and Implications for the Presence of Volatiles

B. W. Denevi,[1]* D. T. Blewett,[1] D. L. Buczkowski,[1] F. Capaccioni,[2] M. T. Capria,[2] M. C. De Sanctis,[2] W. B. Garry,[3] R. W. Gaskell,[3] L. Le Corre,[4] J.-Y. Li,[3,5] S. Marchi,[6] T. J. McCoy,[7] A. Nathues,[4] D. P. O'Brien,[3] N. E. Petro,[8] C. M. Pieters,[9] F. Preusker,[10] C. A. Raymond,[11] V. Reddy,[4,12] C. T. Russell,[13] P. Schenk,[14] J. E. C. Scully,[13] J. M. Sunshine,[5] F. Tosi,[2] D. A. Williams,[15] D. Wyrick[16]

We investigated the origin of unusual pitted terrain on asteroid Vesta, revealed in images from the Dawn spacecraft. Pitted terrain is characterized by irregular rimless depressions found in and around several impact craters, with a distinct morphology not observed on other airless bodies. Similar terrain is associated with numerous martian craters, where pits are thought to form through degassing of volatile-bearing material heated by the impact. Pitted terrain on Vesta may have formed in a similar manner, which indicates that portions of the surface contain a relatively large volatile component. Exogenic materials, such as water-rich carbonaceous chondrites, may be the source of volatiles, suggesting that impactor materials are preserved locally in relatively high abundance on Vesta and that impactor composition has played an important role in shaping the asteroid's geology.

In July 2011, the Dawn spacecraft entered into orbit around Vesta, the second-most massive asteroid in the solar system. After initial Survey and High-Altitude orbits, Dawn spiraled down to its ~210-km Low-Altitude Mapping Orbit (LAMO) (*1*), allowing for acquisition of Framing Camera (FC) images (*2*) at pixel scales of <20 m, as well as high-resolution views of Vesta's geology. LAMO clear-filter images cover >70% of the surface (latitudes above ~55°N were in shadow). In this data set, we identified terrain with a distinct pitted morphology. Here, we describe this terrain and its implications for the presence and origin of volatiles on Vesta.

The most widespread occurrence of pitted terrain is associated with Marcia crater (~70-km diameter, Fig. 1A). Marcia is among the most recent large impacts on Vesta; using the methods of Marchi *et al.* (*3*), we estimate its age to be ~70 million years. Pitted terrain is found on otherwise smooth deposits located on the crater floor surrounding a small central peak, atop a slump terrace, and within portions of the continuous ejecta blanket. Pits lack raised rims, and on the floor they range in size from ~30 m (near the limit of resolution at 17 m per pixel) to just over 1 km in diameter (Fig. 1, B to D). Pits found in clusters on the slump terrace and ejecta blanket are smaller (largest sizes: ~250 m) and are often located where ejecta fills topographic lows (Fig. 1, A and F). On the floor, material that slumped down the crater walls appears to bury the pitted terrain in several areas; in others, pits may occur within the slump deposits (fig. S1). Toward the center of the floor where the deposit is probably thickest, pits increase in size, and their shapes become more

[1]The Johns Hopkins University Applied Physics Laboratory, Laurel, MD, USA. [2]Istituto di Astrofisica e Planetologia Spaziali, Istituto Nazionale di Astrofisica, Rome, Italy. [3]Planetary Science Institute, Tucson, AZ, USA. [4]Max Planck Institute for Solar System Research, Katlenburg-Lindau, Germany. [5]University of Maryland, College Park, MD, USA. [6]NASA Lunar Science Institute, Boulder, CO, USA. [7]National Museum of Natural History, Smithsonian Institution, Washington, DC, USA. [8]NASA Goddard Space Flight Center, Greenbelt, MD, USA. [9]Brown University, Providence, RI, USA. [10]Deutsches Zentrum fur Luft- und Raumfahrt (DLR), Institute of Planetary Research, Berlin, Germany. [11]Jet Propulsion Laboratory, California Institute of Technology, Pasadena, CA, USA. [12]University of North Dakota, Grand Forks, ND, USA. [13]University of California, Los Angeles, CA, USA. [14]Lunar and Planetary Institute, Houston, TX, USA. [15]Arizona State University, Tempe, AZ, USA. [16]Southwest Research Institute, San Antonio, TX, USA.

*To whom correspondence should be addressed. E-mail: brett.denevi@jhuapl.edu

irregular (Fig. 1, C and D). In many places, pits coalesce and overlap, resulting in polygonal boundaries between adjacent pits. A digital terrain model (*4*) derived from LAMO images shows that individual pits are typically <50 m deep (Fig. 1B); the largest pit complex is ~200 m deep.

The floor deposit in which Marcia's pitted terrain resides is relatively flat, apart from a broad region in the southeast that is ~200 m below the rest of the crater floor (Fig. 1B). This region contains both pits and relatively smooth areas; if the crater floor once approximated an equipotential surface, this implies a high degree of subsidence. Around the margins of the broad depression are several slump scarps (Fig. 1E), and we see evidence for subsidence at the edge of a complex pit (Fig. 1D) and surrounding a large isolated pit, where several terraces may indicate successive levels of downslope movement (Fig. 1C).

Pits in the fresh crater Cornelia (15-km diameter, Fig. 2A) have similar morphologies but are restricted to the crater floor (Fig. 2B) and are smaller (<350 m). In some areas, pits abut or form within slumped material (Fig. 2B and fig. S1). Within Licinia crater (24-km diameter, Fig. 2C), the identification of pitted terrain is tentative. The occurrence is limited, with small clusters of pits surrounded by larger expanses of smooth floor material (Fig. 2D). Licinia is slightly more degraded with more superposed impact craters, and pits are not as sharply defined. Pit sizes range from ~30 to 500 m. The floor of Numisia crater (33-km diameter, Fig. 2E) is even more ambiguous, with a small hummocky area that could represent a degraded cluster of pits that are each less than ~600 m across (Fig. 2F). The positive identification of pitted terrain within two of the youngest craters on Vesta suggests that its occurrence may have been more widespread but has degraded or been buried with time.

Marcia, Cornelia, and Numisia craters all have large exposures of dark material (*5*–*7*); Licinia has not been observed at illumination conditions favorable for the assessment of albedo. FC color images and spectra from the Visible and Infrared Spectrometer (VIR) (*8*) show that the floor deposits at Marcia and Cornelia are distinct in color from their surroundings (Fig. 3), with 6 to 13% lower reflectance at 750 nm than average values for Vesta, whereas the dark material at each crater is 35 to 39% lower in reflectance. Pyroxene absorption bands are 4 to 9% shallower in the floor deposit than average for Vesta; local dark material has 15 to 21% shallower bands. VIR emission spectra show that the floor deposits have distinct thermal properties (fig. S2).

Analogous pitted terrain is not observed on other airless bodies (fig. S3), and the lack of alignment and distinct morphology are inconsistent with drainage of material into subsurface fractures (fig. S4). Pitted terrain in more than 200 fresh craters on Mars has similar morphologies (Fig. 4) and corresponding occurrences on floor deposits, terraces, and ejecta (*9*–*13*). Formation models for the martian pitted terrain include collapse due to sublimation of ice long after the impact event (*11*) or erosion due to rapid degassing of volatiles within a melt-breccia mixture heated by the impact event (*12*, *13*). Either scenario

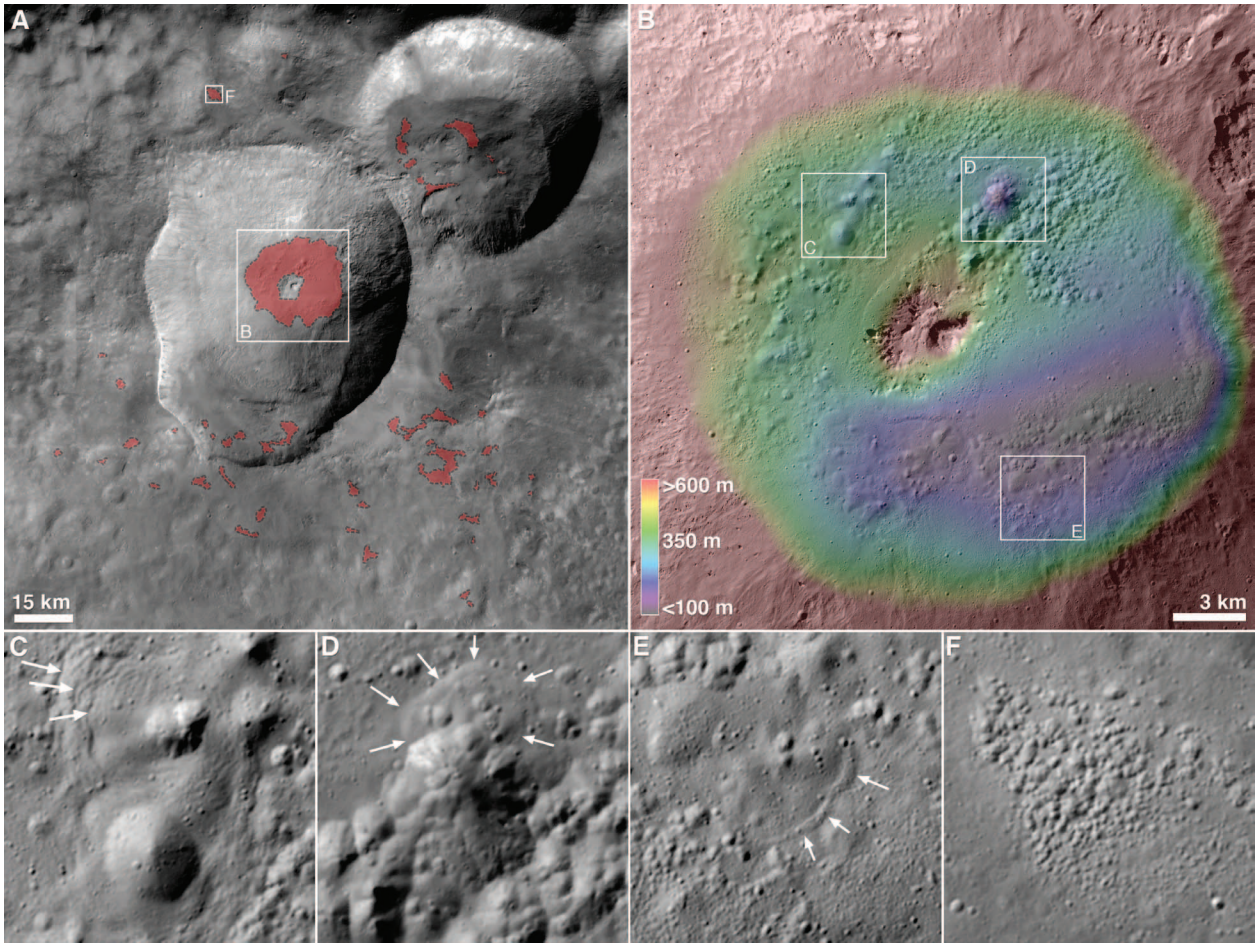

Fig. 1. Clear filter mosaic of pitted terrain at Marcia crater. (**A**) The sharp, raised rim indicates that Marcia is one of the youngest craters on Vesta. Locations of pitted terrain are indicated in red (boundaries approximate). North is toward the top and illumination is from the east in all images. (**B**) The crater floor displays the largest concentration of pits. A colorized digital terrain model derived with elevations calculated relative to a geoid is shown overlaid on a LAMO image mosaic. (**C**) Pits on the floor display successive levels of downslope movement. The top, irregular pit has ripplelike features that may also be constructional [width of (C) to (F) is 3.5 km; locations of (C) to (E) are shown in (B)]. (**D**) Complex pitted terrain where pits share walls in near-polygonal boundaries and appear to coalesce. Arrows indicate a region of subsidence surrounding and overlapping several pits. (**E**) Slump scarp that probably indicates downslope movement due to subsidence. (**F**) A cluster of pits within the ejecta of Marcia [location shown in (A)]. All images were photometrically corrected using the procedure of Reddy *et al*. (*7*).

requires volatiles, presumed to be largely water ice, in substantial abundances [minimum abundance is not well defined; estimates range up to 12 weight percent (wt %) (*12*)].

The marked similarities between pitted terrains on Mars and Vesta suggest a similar origin. However, the prospect of abundant volatiles originating on Vesta is counter to the generally low endogenic volatile contents (*14*) indicated by meteorites thought to originate from Vesta (*15*, *16*), and Vesta's basaltic crust is thought to have degassed (*17*). Thus, the source of volatiles is likely to be exogenic. The association of pitted terrain with craters that have prominent exposures of dark material within their walls and ejecta (Fig. 3) may be a key observation. Telescopic spectra indicate the presence of OH and possibly H_2O on Vesta (*18*, *19*); Dawn's Gamma Ray and Neutron Detector (GRaND) observes a heterogeneous distribution of H across the surface and finds that the highest abundances are associated with broad regions of low albedo (*20*). Carbonaceous chondrites, which have been observed as clasts in howardites (*21*, *22*), are both low in reflectance (*23*) and contain an average of 9 wt % mineralogically bound water (*24*). The spectral properties of dark deposits indicate that carbonaceous material may comprise up to 60% of the regolith (*25*), which would indicate that ~5 wt % H_2O may be present in these areas. Later impacts into this water-bearing regolith would result in devolatilization due to impact heating and melting. Evidence for impact melt is seen at both Marcia and Cornelia (fig. S5),

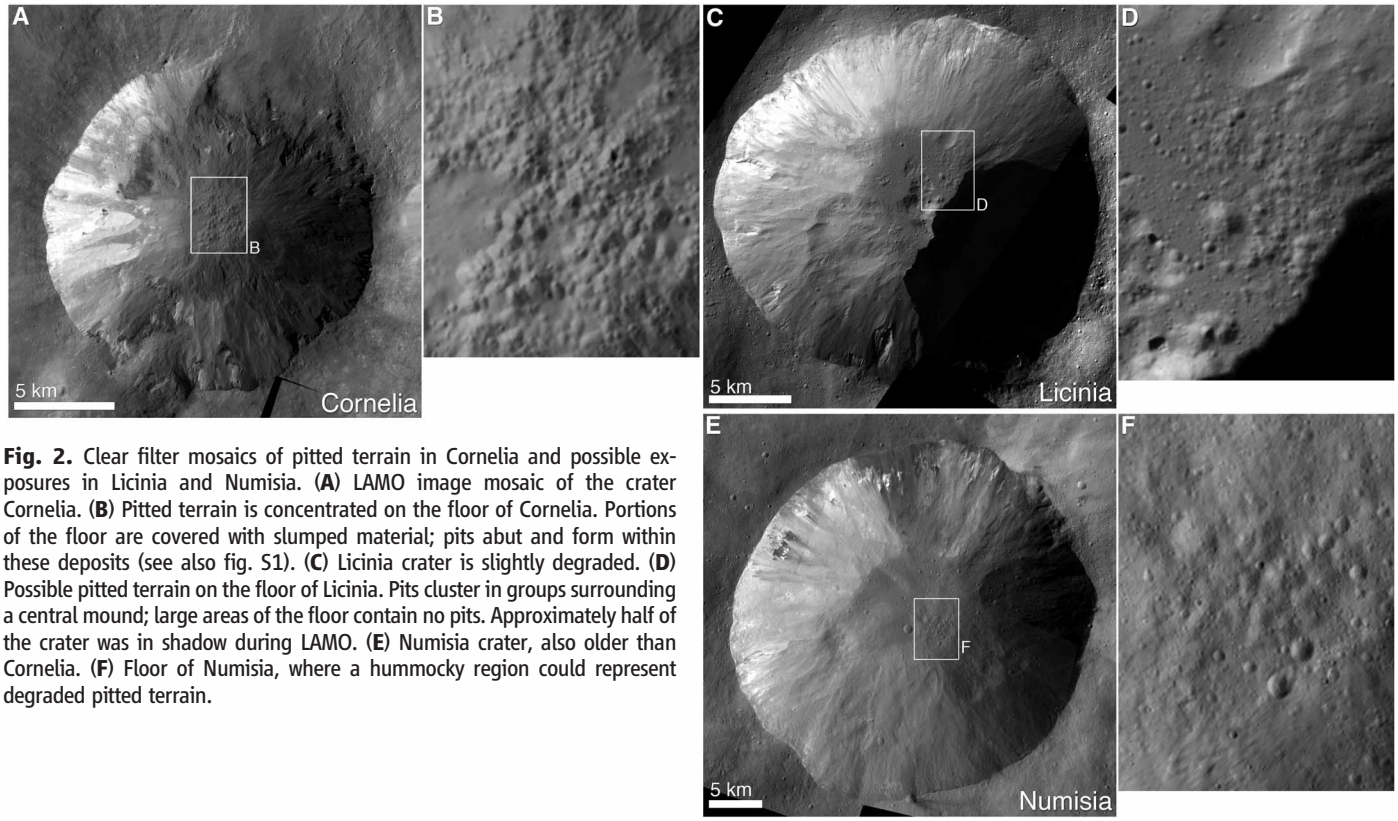

Fig. 2. Clear filter mosaics of pitted terrain in Cornelia and possible exposures in Licinia and Numisia. (**A**) LAMO image mosaic of the crater Cornelia. (**B**) Pitted terrain is concentrated on the floor of Cornelia. Portions of the floor are covered with slumped material; pits abut and form within these deposits (see also fig. S1). (**C**) Licinia crater is slightly degraded. (**D**) Possible pitted terrain on the floor of Licinia. Pits cluster in groups surrounding a central mound; large areas of the floor contain no pits. Approximately half of the crater was in shadow during LAMO. (**E**) Numisia crater, also older than Cornelia. (**F**) Floor of Numisia, where a hummocky region could represent degraded pitted terrain.

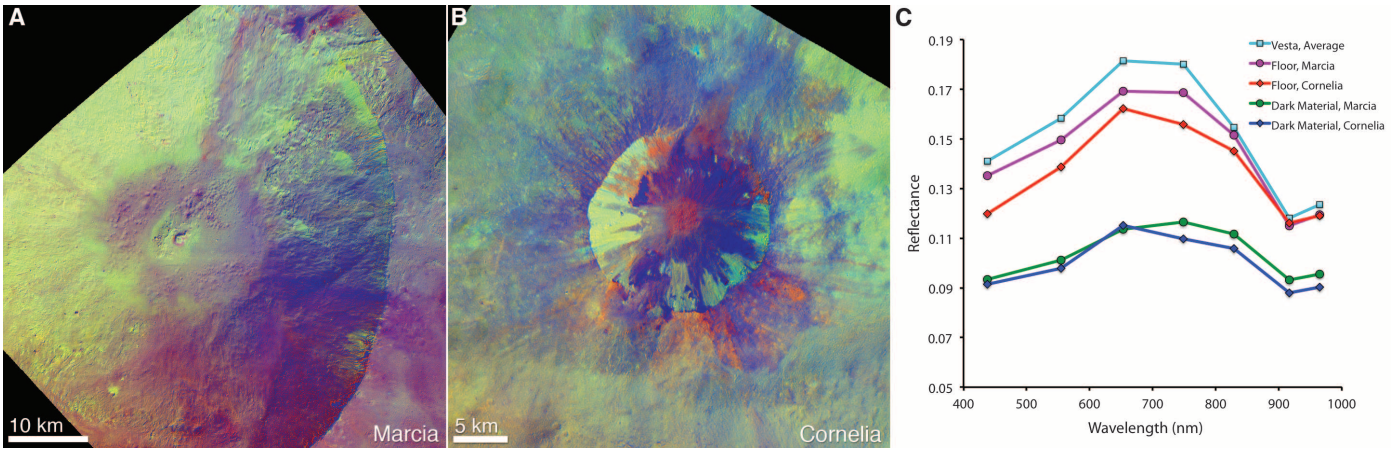

Fig. 3. Spectral properties of Marcia and Cornelia craters. (**A**) Enhanced color view of Marcia crater. Color is displayed with 749/438 nm in red, 749/917 nm in green, and 438/749 nm in blue and is shown overlaid on a 749-nm image to retain morphologic information. In this color scheme, green areas indicate stronger absorption bands and red areas indicate steeper spectral slopes. Dark material, with shallow absorption bands and spectral slopes, is observed at both craters and is shown in blue. (**B**) Enhanced color view of Cornelia crater with the same color scheme. The floors of both craters are distinct from their surroundings, suggesting a difference in physical properties or composition. (**C**) Spectra of the floors and local dark material at Marcia and Cornelia, shown with an average spectrum of Vesta for comparison.

and pit formation via dehydration is consistent with GRaND observations of lower H abundances immediately surrounding Marcia crater (*20*).

Rapid degassing of a volatile-bearing melt-breccia mixture is consistent with the observed morphologies of Vesta's pitted terrain. Slumping around some pits (Fig. 1) may be due to terrain being undercut as material is eroded during pit development. Pits that formed within the edges of crater wall slumps (fig. S1) may have continued to degas through the slumped material. Where wall slumps were thicker, they probably inhibited pit formation. Fresh craters with flat floor deposits, like those that host the pitted terrain, are rare on Vesta. Other large craters that expose dark material are either substantially more degraded or their formation on relatively steep slopes resulted in large, asymmetric slump deposits (*5*) that buried what would have been the crater floor. The sizes of pits on Vesta follow the Mars power-law trend of increasing pit size with host crater diameter (*13*). Pit size appears to be controlled by the thickness of the impact-heated deposit, expected to be similar on both bodies, rather than specific volatile content.

An alternative source of volatiles is impacting comets. As ice is not likely to be stable in sufficient volumes near Vesta's surface at equatorial latitudes (*26*), cometary volatiles would need to be delivered during the crater-forming event. However, the high impact velocities of comets typically result in vaporization and loss of the majority of the projectile, which suggests that little cometary material would be preserved within the crater floor and local ejecta. We also see evidence that pitted terrain may be tied to local surface properties rather than specific impactor composition. Though a small sample, pitted terrain is located only in regions not associated with the Rheasilvia impact basin, which dominates Vesta's southern hemisphere (*27*) and contains the lowest concentrations of hydrogen (*20*) and a dearth of dark material (*6*).

The formation mechanism for pitted terrain must explain the occurrence of these features on Mars and Vesta and their absence on the Moon, Mercury, and other asteroids for which images of comparable resolution exists. If delivery of hydrated material to the surface by impactors such as carbonaceous chondrites can result in the development of pitted terrain, similar features should be observed on other volatile-poor airless bodies. Higher average impact velocities at Mercury and the Moon (*28*) may account for this difference, reducing the likelihood that impactors will be preserved without shock devolatilization. Pitted terrain may yet be discovered on other asteroids; among the handful already imaged at high resolution, the large size, complex geologic evolution, and chance collisional history of Vesta set it apart. Vesta's surface appears to be unique among airless bodies observed to date in the nature and degree of preservation of exogenic materials.

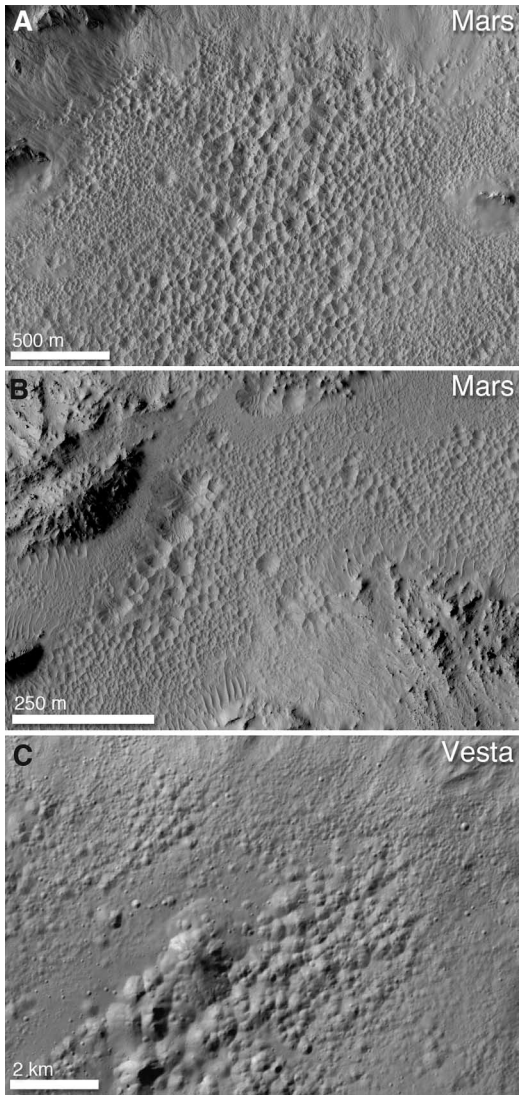

Fig. 4. Comparison between pitted terrain on Mars and Vesta. The morphologies of pits are similar, with irregular shapes and near-polygonal margins where pits share walls. (**A**) Floor of the 28-km crater Tooting, Mars [23.2°N, 207.8°E; High Resolution Imaging Science Experiment (HiRISE) image 1538_2035]. (**B**) The 10-km Zunil crater, Mars (7.7°N, 166.2°E; HiRISE image 1764_1880). (**C**) Marcia crater, Vesta. Whereas the examples shown here are at different scales, pits on Vesta fall on the martian trend for pit size versus crater diameter (*13*).

References and Notes

1. C. T. Russell, C. A. Raymond, *Space Sci. Rev.* **163**, 3 (2011).
2. H. Sierks *et al.*, *Space Sci. Rev.* **163**, 263 (2011).
3. S. Marchi *et al.*, *Science* **336**, 690 (2012).
4. R. W. Gaskell *et al.*, *Meteorit. Planet. Sci.* **43**, 1049 (2008).
5. R. Jaumann *et al.*, *Science* **336**, 687 (2012).
6. T. B. McCord *et al.*, abstract no. 1352, 43rd Annual Lunar and Planetary Science Conference, The Woodlands, TX, 19 to 23 March 2012.
7. V. Reddy *et al.*, *Science* **336**, 700 (2012).
8. M. C. De Sanctis *et al.*, *Space Sci. Rev.* **163**, 329 (2011).
9. A. S. McEwen *et al.*, *Science* **317**, 1706 (2007).
10. P. J. Mouginis-Mark, H. Garbeil, *Meteorit. Planet. Sci.* **42**, 1615 (2007).
11. W. K. Hartmann, C. Quantin, S. C. Werner, O. Popova, *Icarus* **208**, 621 (2010).
12. J. M. Boyce, L. Wilson, P. J. Mouginis-Mark, C. W. Hamilton, L. L. Tornabene, *Icarus* **221**, 262 (2012).
13. L. L. Tornabene *et al.*, *Icarus* **220**, 348 (2012).
14. D. W. Mittlefehldt, T. J. McCoy, C. A. Goodrich, A. Kracher, in *Planetary Materials*, J. J. Papike, Ed. (Mineralogical Society of America, Washington, DC, 1998), pp. 4-1–4-196.
15. T. B. McCord, J. B. Adams, T. V. Johnson, *Science* **168**, 1445 (1970).
16. R. P. Binzel, S. Xu, *Science* **260**, 186 (1993).
17. L. Wilson, K. Keil, *J. Geophys. Res.* **101**, 18927 (1996).
18. S. Hasegawa *et al.*, *Geophys. Res. Lett.* **30**, 2123 (2003).
19. A. S. Rivkin, L. A. McFadden, R. P. Binzel, M. Sykes, *Icarus* **180**, 464 (2006).
20. T. H. Prettyman *et al.*, *Science* **338**, 242 (2012); 10.1126/science.1225354.
21. A. E. Rubin, W. F. Bottke, *Meteorit. Planet. Sci.* **44**, 701 (2009).
22. J. S. Herrin, M. E. Zolensky, J. A. Cartwright, D. W. Mittlefehldt, D. K. Ross, abstract no. 2806, 42nd Annual Lunar and Planetary Science Conference, The Woodlands, TX, 7 to 11 March 2011.
23. E. A. Cloutis, P. Hudon, T. Hiroi, M. J. Gaffey, P. Mann, *Icarus* **216**, 309 (2011).
24. A. E. Rubin, J. M. Trigo-Rodriguez, H. Huber, J. T. Wasson, *Geochim. Cosmochim. Acta* **71**, 2361 (2007).
25. V. Reddy *et al.*, abstract no. 1587, 43rd Annual Lunar and Planetary Science Conference, The Woodlands, TX, 19 to 23 March 2012.
26. F. P. Fanale, J. R. Salvail, *Icarus* **82**, 97 (1989).
27. P. Schenk *et al.*, *Science* **336**, 694 (2012).
28. M. Le Feuvre, M. A. Wieczorek, *Icarus* **197**, 291 (2008).

Acknowledgments: We thank the Dawn Science, Instrument, and Operations Teams and the Dawn at Vesta Participating Scientist program for support. A portion of this work was performed at the Jet Propulsion Laboratory, California Institute of Technology, under contract with NASA, and portions were supported by the Italian Space Agency. Dawn data are archived with the NASA Planetary Data System.

Supplementary Materials

www.sciencemag.org/cgi/content/full/science.1225374/DC1
Figs. S1 to S5
References (*29–33*)

30 May 2012; accepted 28 August 2012
Published online 20 September 2012;
10.1126/science.1225374